Implementing Transverse Momentum Dependent splitting functions in Parton Branching evolution equations

Lissa Keersmaekers⋆

University of Antwerp

⋆ lissa.keersmaekers@uantwerpen.be

Proceedings for the XXVIII International Workshop on Deep-Inelastic Scattering and Related Subjects, Stony Brook University, New York, USA, 12-16 April 2021

Abstract

The Parton Branching (PB) approach describes the evolution of transverse momentum dependent (TMD) parton densities. We propose to extend the PB method by including TMD splitting functions, instead of the DGLAP splitting functions which assume strong ordering in transverse momentum. We present the evolution equations and their numerical solution, which is the first Monte Carlo implementation including TMD splitting functions.

1 Introduction

TMD factorization theorems (see [1] and references therein) are important for precise theoretical predictions of physical observables such as the Drell-Yan (DY) transverse momentum spectrum in hadronic collisions. The Parton Branching (PB) method [2–4] allows one to obtain the evolution of TMD Parton Distribution Functions (TMD PDFs) in terms of Sudakov form factors, real-emission splitting functions and angular-ordering phase space constraints. The method has recently been applied to DY [5–7] and photon-induced [8] lepton-pair production, and to DY + jets production [9]. It has been implemented in the Monte Carlo (MC) event generator CASCADE [10, 11].

Currently, the PB method uses Dokshitzer-Gribov-Lipatov-Altarelli-Parisi (DGLAP) [12–14] splitting functions, which assume that the partons along the branching decay chain are strongly ordered in transverse momenta. From high-energy factorization [15–17], it is known that potentially large corrections to strongly-ordered branchings arise for small longitudinal-momentum fractions x [18, 19]. These corrections can be taken into account by generalizing the concept of DGLAP splitting functions to that of TMD splitting functions [20, 21]. A calculational programme of TMD splitting functions is pursued in [22–26].

We propose in this work an implementation of TMD splitting functions within the PB method. It is the first MC implementation that uses TMD splitting functions and a first step towards a new MC that includes small-x physics.

2 Evolution equations

In this work, three different scenarios for PB evolution equations are studied [27]. The equations for momentum-weighted TMD PDFs $\tilde{\mathcal{A}}_a(x, \boldsymbol{k}, \mu^2) = x\tilde{\mathcal{A}}_a(x, \boldsymbol{k}, \mu^2)$ for a parton of flavour a, evaluated at a scale μ, with x the longitudinal momentum fraction of the proton and $\boldsymbol{k}$ the transverse momentum, are given by

$$\tilde{\mathcal{A}}_a(x, \boldsymbol{k}, \mu^2) = \Delta_a(\mu^2)\tilde{\mathcal{A}}_a(x, \boldsymbol{k}, \mu_0^2) + \sum_b \int \frac{d^2\boldsymbol{\mu}'}{\pi\mu'^2} \frac{\Delta_a(\mu^2)}{\Delta_a(\mu'^2)}\Theta(\mu^2 - \mu'^2)\Theta(\mu'^2 - \mu_0^2) \times$$
$$\times \int_x^{z_M} dz P_{ab}\tilde{\mathcal{A}}_b(\frac{x}{z}, \boldsymbol{k} + (1-z)\boldsymbol{\mu}', \mu'^2), \tag{1}$$

where Δ_a is the Sudakov form factor for parton a, P_{ab} is the real-emission function for parton splitting $b \to a$, and the phase-space angular ordering is embodied in i) the running coupling, ii) the relationship between the evolution variable and the transverse momentum, and iii) the soft gluon resolution scale z_M. The latter separates resolvable from non-resolvable branchings, and is taken to be dynamical, i.e., dependent on the evolution scale μ': $z_M = 1 - q_0/\mu'$, where the parameter q_0 represents the minimal transverse momentum of the emitted parton. The main features of this approach are described in [6]. The three scenarios are characterized as follows:

1. $P_{ab} = P_{ab}^{col}(z, \mu'^2)$ and $\Delta_a(\mu^2) = \Delta_a^{col}(\mu^2)$;

2. $P_{ab} = P_{ab}^{TMD}(z, \boldsymbol{k}', \boldsymbol{\mu}')$, with $\boldsymbol{k}' = \boldsymbol{k} + (1-z)\boldsymbol{\mu}'$, and $\Delta_a(\mu^2) = \Delta_a^{col}(\mu^2)$;

3. $P_{ab} = P_{ab}^{TMD}(z, \boldsymbol{k}', \boldsymbol{\mu}')$ and $\Delta_a(\mu^2) = \Delta_a^{TMD}(\mu^2, \boldsymbol{k}^2)$.

The resolvable branching probabilities of the first condition $P_{ab}^{col}(z, \mu'^2)$ are the real emission parts of the DGLAP splitting functions. The TMD splitting functions in their original variables $\breve{P}_{ab}^R(z, \boldsymbol{k}', \tilde{\boldsymbol{k}})$, which can be found in [25], are defined within the 2-gluon irreducible kernels, which integrate over the boost-invariant transverse momentum $\tilde{\boldsymbol{k}} = \boldsymbol{k} - z\boldsymbol{k}'$. For the second and third condition we use the TMD splitting functions $P_{ab}^{TMD}(z, \boldsymbol{k}', \boldsymbol{\mu}') = \frac{d^2\tilde{\boldsymbol{k}}}{\tilde{\boldsymbol{k}}^2}\frac{\mu'^2}{d^2\mu'}\breve{P}_{ab}^R(z, \boldsymbol{k}', \tilde{\boldsymbol{k}})$, were we have chosen to absorb a Jacobian in their redefinition. The collinear Sudakov form factor, which resums non-resolvable branchings and virtual corrections, is given by
$\Delta_a^{col}(\mu^2) = \exp[-\sum_b \int_{\mu_0^2}^{\mu^2} \frac{d\mu'^2}{\mu'^2} \int_0^{z_M} dz \, z \, P_{ba}^{col}(z, \mu'^2)]$. In the standard PB method, which corresponds to the first condition, it has the interpretation of the probability of an evolution without any resolvable branching. Since we change the resolvable branching probabilities in the second condition, this interpretation is no longer valid. In the third condition the TMD Sudakov form factor $\Delta_a^{TMD}(\mu^2, \boldsymbol{k}^2) = \exp[-\sum_b \int_{\mu_0^2}^{\mu^2} \frac{d\mu'^2}{\mu'^2} \int_0^{2\pi} \frac{d\phi}{2\pi} \int_0^{z_M} dz \, z \, P_{ba}^{TMD}(z, \boldsymbol{k}, \mu')]$, where ϕ is the angle between $\boldsymbol{k}$ and $\boldsymbol{\mu}'$, is defined such that this interpretation is again valid. This condition has effects of TMD splitting functions in both resolvable and non-resolvable branchings. At $\boldsymbol{k} = 0$, the TMD Sudakov form factor is equal to the collinear Sudakov form factor. When $\boldsymbol{k}$ increases, the TMD Sudakov form factors decrease for both gluons and quarks.
A property of the equations with the first and third condition is that the momentum of the

Table 1: Check of momentum conservation: $\int_{10^{-5}}^{1} dx \, \tilde{f}_a(x, \mu^2)$.

μ^2 (GeV)	$P_{ab}^{col}, \Delta_a^{col}$ (condition 1)	$P_{ab}^{TMD}, \Delta_a^{col}$ (condition 2)	$P_{ab}^{TMD}, \Delta_a^{TMD}$ (condition 3)
10	0.999	1.007	0.999
100	0.997	1.045	0.997
1000	0.995	1.091	0.994
10000	0.992	1.129	0.991
100000	0.984	1.148	0.983

proton is conserved. The second condition doesn't conserve the proton's momentum. This can be shown analytically, and is shown numerically in table 1.

The evolution equations are here shown for TMD PDFs, but to obtain collinear PDFs, one can simply integrate over the transverse momentum $\boldsymbol{k}$: $\tilde{f}_a(x, \mu^2) = \int \frac{d^2 \boldsymbol{k}}{\pi} \tilde{\mathcal{A}}_a(x, \boldsymbol{k}, \mu^2)$.

The equations can be solved with MC techniques.

3 Numerical results

In this section, we show results for the evolution equations 1 obtained with the same initial parametrization for all scenarios $\tilde{\mathcal{A}}_a(x, k_{\perp,0}, \mu_0^2) = x f_a(x, \mu_0^2) \cdot \frac{1}{q_s^2} \exp\left(-k_{\perp,0}^2/q_s^2\right)$ at scale $\mu_0^2 = 1.9$ GeV^2. The x-dependence is generated according to a collinear PDF $x f_a(x, \mu_0^2)$ which is chosen to HERAPDF20_LO_EIG and the $k_\perp$-dependence is generated according to a Gaussian, with $q_s = 0.5$ GeV. By using fixed starting distributions, we can study the impact of each element in the evolution equations. However, before the TMD PDFs can be applied to phenomenology, they should be fitted, which is left for future work. In figure 1, we show the gluon distribution at scale $\mu = 100$ GeV obtained with condition 1 (col P), condition 2 (TMD P col Sud) and condition 3 (TMD P TMD Sud). The bottom plots show the ratio between the different curves, compared to condition 1. With these ratio plots one can easily see the differences between the evolved TMDs in the whole x or $k_\perp$ region. Left, the integrated TMD PDF versus x is shown. The TMD splitting functions affect the distributions already at the level of integrated TMDs. The TMD splitting functions reduce to the DGLAP splitting functions for $\boldsymbol{k}' \to 0$ and therefore the effects of them are small in the large-x region. A suppression in the PDF can be seen for the model with TMD Sudakov form factor compared to the PDF from the model that uses TMD splitting functions and a collinear Sudakov form factor. Right, the TMD PDF versus $k_\perp$ at $x = 0.001$ is shown. The whole $k_\perp$-region is affected by the TMD splitting functions. The suppression from the TMD Sudakov form factor is visible in the whole $k_\perp$-region. There are kinks visible in the $k_\perp$-spectrum due to the non-perturbative input.

In figure 2 we show the influence of non-perturbative input. We do this for the first condition, but condition 3 gives similar results. The transverse momentum of a parton after n branchings is given by $\boldsymbol{k} = \boldsymbol{k}_0 - \sum_{i=1}^{n} \boldsymbol{q}_i$, with $\boldsymbol{q}_i = (1-z)\boldsymbol{\mu}_i$ the transverse momentum of the emitted parton. Since we use the dynamical resolution scale, we have $q_{\perp,i} > q_0$ and the transverse momentum from the evolution begins to build up around the value of q_0. But since we have a vector sum, $k_\perp$ below q_0 can be reached and the peak can be smeared by many branchings. In the left figure we show the gluon TMD PDF vs $k_\perp$ for different values of q_0. We see that when we lower q_0, the curve gets smoother, this has two reasons: with low q_0 there are more
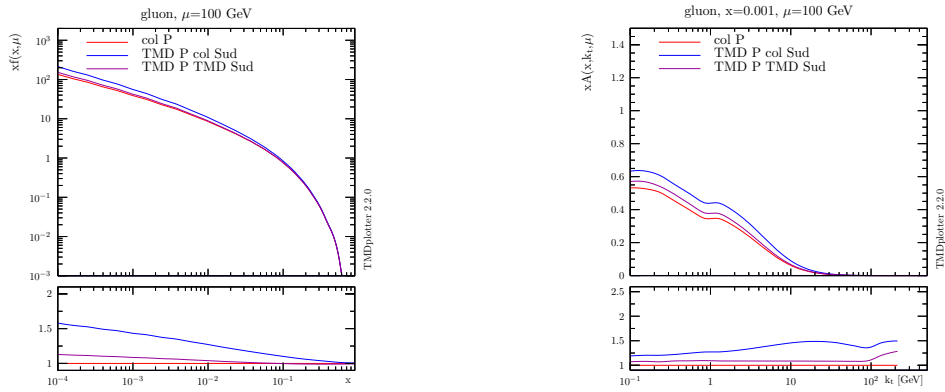
Figure 1: Collinear (left) and TMD (right) PDFs for gluons. The bottom plots show the ratio between the curves.
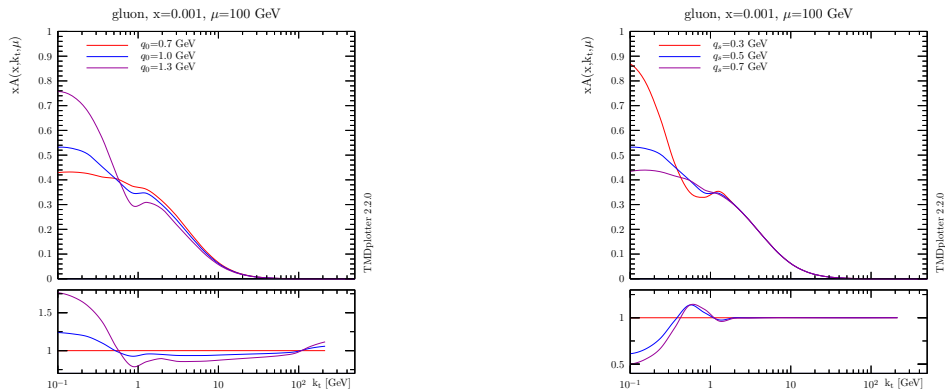
Figure 2: Gluon TMD PDFs for different values of the non-perturbative input q_0 and q_s. The bottom plots show the ratio between the curves.

resolvable branchings and therefore the peak from evolution is more smeared out and with low q_0 the overlap is larger with the peak from intrinsic $k_\perp$ around 0. In the right figure we show the effects of the width of the Gaussian function for intrinsic $k_\perp$, by varying q_s, while q_0 is fixed at 1 Gev. When q_s is close to q_0, the curve is smoother than when q_s is smaller, again because of the overlap between the two peaks. We can see that q_s only affects the small $k_\perp$-region.

4 Conclusion

We have presented a Monte Carlo implementation of TMD splitting functions in the Parton Branching approach. The TMD splitting functions affect both resolvable branchings and Sudakov form factors. The evolution with TMD splitting functions has impact on both collinear and TMD parton distributions. The effects are visible in the small-x region of PDFs and throughout the whole $k_\perp$-spectrum of TMD PDFs. Phenomenological studies are warranted at the LHC as well as at future hadron-hadron [28, 29] and lepton-hadron [30, 31] colliders.

Acknowledgements

I thank Francesco Hautmann, Martin Hentschinski, Hannes Jung, Aleksander Kusina, Krzysztof Kutak and Aleksandra Lelek for collaboration and discussion.

References

[1] R. Angeles-Martinez et al., *Transverse Momentum Dependent (TMD) Parton Distribution Functions: Status and Prospects*, Acta Phys. Pol. B **46**, 2501 (2015), doi:10.5506/APhysPolB.46.2501.

[2] F. Hautmann, H. Jung, A. Lelek, V. Radescu and R. Žlebčík, *Soft-gluon resolution scale in QCD evolution equations*, Phys. Lett. B **772**, 446 (2017), doi:10.1016/j.physletb.2017.07.005.

[3] F. Hautmann, H. Jung, A. Lelek, V. Radescu and R. Žlebčík, *Collinear and TMD quark and gluon densities from parton branching solution of QCD evolution equations*, J. High Energy Phys. **01**, 070 (2018), doi:10.1007/JHEP01(2018)070.

[4] A. Bermudez Martinez, P. Connor, H. Jung, A. Lelek, R. Žlebčík, F. Hautmann and V. Radescu, *Collinear and TMD parton densities from fits to precision DIS measurements in the parton branching method*, Phys. Rev. D **99**, 074008 (2019), doi:10.1103/PhysRevD.99.074008.

[5] A. Bermudez Martinez et al., *Production of z bosons in the parton branching method*, Phys. Rev. D **100**, 074027 (2019), doi:10.1103/PhysRevD.100.074027.

[6] F. Hautmann, L. Keersmaekers, A. Lelek and A. M. van Kampen, *Dynamical resolution scale in transverse momentum distributions at the LHC*, Nucl. Phys. B **949**, 114795 (2019), doi:10.1016/j.nuclphysb.2019.114795.

[7] A. Bermudez Martinez et al., *The transverse momentum spectrum of low mass Drell–Yan production at next-to-leading order in the parton branching method*, Eur. Phys. J. C **80**, 598 (2020), doi:10.1140/epjc/s10052-020-8136-y.

[8] H. Jung, S. Taheri Monfared and T. Wening, *Determination of collinear and TMD photon densities using the Parton Branching method*, Phys. Lett. B **817**, 136299 (2021), doi:10.1016/j.physletb.2021.136299.

[9] A. Bermudez Martinez, F. Hautmann and M. L. Mangano, *TMD evolution and multi-jet merging*, Phys. Lett. B **822**, 136700 (2021), doi:10.1016/j.physletb.2021.136700.

[10] S. Baranov et al., *CASCADE3 A Monte Carlo event generator based on TMDs*, Eur. Phys. J. C **81**, 425 (2021), doi:10.1140/epjc/s10052-021-09203-8.

[11] H. Jung et al., *The CCFM Monte Carlo generator CASCADE Version 2.2.03*, Eur. Phys. J. C **70**, 1237 (2010), doi:10.1140/epjc/s10052-010-1507-z.

[12] V. N. Gribov and L. N. Lipatov, *Deep inelastic e p scattering in perturbation theory*, Sov. J. Nucl. Phys. **15**, 438 (1972).

[13] G. Altarelli and G. Parisi, *Asymptotic freedom in parton language*, Nucl. Phys. B **126**, 298 (1977), doi:10.1016/0550-3213(77)90384-4.

[14] Y. L. Dokshitzer, *Calculation of the Structure Functions for Deep Inelastic Scattering and e+ e- Annihilation by Perturbation Theory in Quantum Chromodynamics.*, Sov. Phys. JETP **46**, 641 (1977).

[15] S. Catani, M. Ciafaloni and F. Hautmann, *Gluon contributions to small x heavy flavour production*, Phys. Lett. B **242**, 97 (1990), doi:10.1016/0370-2693(90)91601-7.

[16] S. Catani, M. Ciafaloni and F. Hautmann, *High energy factorization and small-x heavy flavour production*, Nucl. Phys. B **366**, 135 (1991), doi:10.1016/0550-3213(91)90055-3.

[17] S. Catani, M. Ciafaloni and F. Hautmann, *High-energy factorization in QCD and minimal subtraction scheme*, Phys. Lett. B **307**, 147 (1993), doi:10.1016/0370-2693(93)90204-U.

[18] F. Hautmann, M. Hentschinski and H. Jung, *TMD PDFs: a Monte Carlo implementation for the sea quark distribution*, arXiv:1205.6358.

[19] F. Hautmann, M. Hentschinski and H. Jung, *A k_T-dependent sea-quark density for the CASCADE Monte Carlo event generator*, arXiv:1207.6420.

[20] S. Catani and F. Hautmann, *High-energy factorization and small-x deep inelastic scattering beyond leading order*, Nuclear Physics B **427**(3), 475 (1994), doi:https://doi.org/10.1016/0550-3213(94)90636-X.

[21] S. Catani and F. Hautmann, *Quark anomalous dimensions at small x*, Phys. Lett. B **315**, 157 (1993), doi:10.1016/0370-2693(93)90174-G.

[22] F. Hautmann, M. Hentschinski and H. Jung, *Forward Z-boson production and the unintegrated sea quark density*, Nucl. Phys. B **865**, 54 (2012), doi:10.1016/j.nuclphysb.2012.07.023.

[23] O. Gituliar, M. Hentschinski and K. Kutak, *Transverse-momentum-dependent quark splitting functions in k_T-factorization: real contributions*, J. High Energy Phys. **01**, 181 (2016), doi:10.1007/JHEP01(2016)181.

[24] M. Hentschinski, A. Kusina and K. Kutak, *Transverse momentum dependent splitting functions at work: Quark-to-gluon splitting*, Phys. Rev. D **94**, 114013 (2016), doi:10.1103/PhysRevD.94.114013.

[25] M. Hentschinski, A. Kusina, K. Kutak and M. Serino, *TMD splitting functions in k_T factorization: the real contribution to the gluon-to-gluon splitting*, Eur. Phys. J. C **78**, 174 (2018), doi:10.1140/epjc/s10052-018-5634-2.

[26] M. Hentschinski, *Transverse momentum dependent gluon distribution within high energy factorization at next-to-leading order*, Phys. Rev. D **104**, 054014 (2021), doi:10.1103/PhysRevD.104.054014.

[27] L. Keersmaekers et al., *paper in preparation* .

[28] M. L. Mangano et al., *Physics at a 100 TeV pp Collider: Standard Model Processes* (2016), doi:10.23731/CYRM-2017-003.1.

[29] P. Azzi et al., *Report from Working Group 1: Standard Model Physics at the HL-LHC and HE-LHC*, CERN Yellow Rep. Monogr. **7**, 1 (2019), doi:10.23731/CYRM-2019-007.1.

[30] P. Agostini et al., *The Large Hadron–Electron Collider at the HL-LHC*, J. Phys. G: Nucl. Part. Phys. **48**, 110501 (2021), doi:10.1088/1361-6471/abf3ba.

[31] Edited by A. Prokudin, Y. Hatta, Y. Kovchegov and C. Marquet,*Probing Nucleons and Nuclei in High Energy Collisions: Dedicated to the Physics of the Electron Ion Collider*, In Proceedings of INT Program INT-18-3, World Scientific, doi:10.1142/11684.